

## Stimulated terahertz emission due to electronic Raman scattering in silicon

S. G. Pavlov,<sup>1,a)</sup> U. Böttger,<sup>1</sup> J. N. Hovenier,<sup>2</sup> N. V. Abrosimov,<sup>3</sup> H. Rijmann,<sup>3</sup>  
R. Kh. Zhukavin,<sup>4</sup> V. N. Shastin,<sup>4</sup> B. Redlich,<sup>5</sup> A. F. G. van der Meer,<sup>5</sup> and H.-W. Hübers<sup>1</sup>

<sup>1</sup>*Institute of Planetary Research, German Aerospace Center (DLR), Rutherfordstraße 2, 12489 Berlin, Germany*

<sup>2</sup>*Kavli Institute of Nanoscience Delft, Delft University of Technology, 2600 GA Delft, The Netherlands*

<sup>3</sup>*Leibniz Institute of Crystal Growth, Max-Born-Straße 2, 12489 Berlin, Germany*

<sup>4</sup>*Institute for Physics of Microstructures, Russian Academy of Sciences, 603950 Nizhny Novgorod, Russia*

<sup>5</sup>*FOM, Institute for Plasma Physics, 3439 MN Nieuwegein, The Netherlands*

(Received 11 March 2009; accepted 26 March 2009; published online 30 April 2009)

Stimulated Raman emission in the terahertz frequency range (4.8–5.1 THz and 5.9–6.5 THz) has been realized by optical excitation of arsenic donor centers in silicon at low temperatures. The Stokes shift of the observed laser emission is 5.42 THz which is equal to the Raman-active donor electronic transition between the ground  $1s(A_1)$  and the excited  $1s(E)$  arsenic states. Optical thresholds of the Raman laser are similar to those observed for other silicon donor lasers. In addition, intracenter donor lasing has been observed when pumping on the dipole-forbidden  $1s(A_1) \rightarrow 2s$  transition. © 2009 American Institute of Physics. [DOI: 10.1063/1.3119662]

Silicon-based semiconductors are intensively investigated over the past years as promising candidates for optoelectronic devices at terahertz frequencies.<sup>1</sup> Major advantages of silicon as a material for terahertz optical components are high thermal conductivity, excellent dielectric properties of its native oxide, and very low optical loss. Intersubband transitions in band structure engineered silicon-based heterostructures,<sup>2,3</sup> transitions between localized states in bulk silicon<sup>4,5</sup> and low-dimensional structures<sup>6,7</sup> have been explored as silicon based THz emitters.

Two types of silicon lasers have been realized so far in the terahertz range. Direct optical transitions between shallow levels of different group-V dopants (P, As, Sb, and Bi) have been used for silicon donor lasers operating under optical pumping at low lattice temperatures.<sup>4,8,9</sup> Stimulated inelastic scattering of light on donor centers in silicon doped by antimony (Si:Sb) and phosphorus (Si:P) has been used for realization of terahertz intracenter Raman lasers.<sup>10,11</sup> These are different from the infrared Raman laser<sup>12,13</sup> which is based on conversion of infrared light in the silicon lattice due to scattering by optical phonons. A major feature of the previously reported intracenter Raman lasers is that light scattering occurs on two lower donor states, which are quiresonantly coupled via the intervalley transverse acoustic  $g$ -phonon. This interaction significantly enhances scattering efficiency and Raman gain.

In this article we report the realization of a terahertz Raman silicon intracenter laser based on inelastic electronic scattering in silicon doped by arsenic (Si:As). Unlike in Si:Sb and Si:P Raman lasers, there are no principal phonons coupling the lower donor states of Si:As and the Raman process relies completely on electronic interactions. It should be noted that Si:As is a very peculiar terahertz laser material because of a strong interaction between the  $2s$  state and the  $1s(A_1)$  ground state via a quiresonant longitudinal acoustic  $f$ -LA intervalley phonon.<sup>14</sup> Evidence of a non-cascade intra-

center relaxation in Si:As has been found.<sup>15</sup> In this letter we report on a Si:As Raman-type laser (Fig. 1) and identify the conditions under which Raman lasing or donor lasing prevails. The influence of the  $2s$  state on the lasing process is analyzed.

The preparation of silicon samples, experimental setup and FEL settings were similar to those in Ref. 11. The silicon crystal has been grown by the float zone technique in [100] direction and doped from the melt with a donor concentration of  $N_D \approx 3 \times 10^{15} \text{ cm}^{-3}$ . The compensation is  $N_A/N_D < 0.001$ , where  $N_A$  is a residual acceptor concentration in the crystal. The sample was chemically-optically polished into a rectangular parallelepiped with dimensions of  $7 \times 7 \times 5 \text{ mm}^3$ . The Si:As sample was mounted in a cryogenic dipstick and cooled down to 4.2 K in a liquid helium (lHe) transport dewar. We used radiation of the tunable free electron laser (FEL) (at the IR-User Facility at the FOM Institute for Plasma Physics) for optical pumping. The FEL generates in the range from  $20 \mu\text{m}$  to  $32 \mu\text{m}$  (9–15 THz, 37–62 meV). All pump energy values given in this publication are readout from the Joule-meter at the entrance of the 10 mm-diameter lightpipe of the dipstick. Optical losses inside the lightpipe are estimated as  $\sim 15 \text{ dB}$ . The spectrum of the FEL emission pulse had a Lorentzian shape with a full width at half maximum (FWHM) of about  $0.14 \mu\text{m}$  ( $\sim 0.1 \text{ meV}$ ). The accuracy of the central wavelength of the FEL pump pulse was  $\sim 0.06 \mu\text{m}$  ( $\sim 0.04 \text{ meV}$ ). A combination of a cold 1 mm thick  $\text{Al}_2\text{O}_3$  filter and a 1 mm thick  $\text{CaF}_2$  filter blocked pump emission toward the lHe cooled Ge:Ga photoconductive detector inside the dipstick (inset in Fig. 2). The emission from the Si:As sample was collected into a Fourier transform spectrometer (FTS) with a resolution of  $\sim 0.05\text{--}0.06 \text{ meV}$ .

Stimulated emission has been obtained for the cases of resonant and nonresonant intracenter pumping. Two typical emission spectra of the Si:As laser are shown in Fig. 1. Pumping with a photon energy of 47.96 meV, which does not correspond to any intracenter transition, yields a single emission line and a single emission pulse. It is similar to what has been observed for Si:Sb and Si:P Raman lasers. This signal

<sup>a)</sup> Author to whom correspondence should be addressed. Tel.: +49 30 67055594. FAX: +49 30 67055507. Electronic mail: sergeij.pavlov@dlr.de.

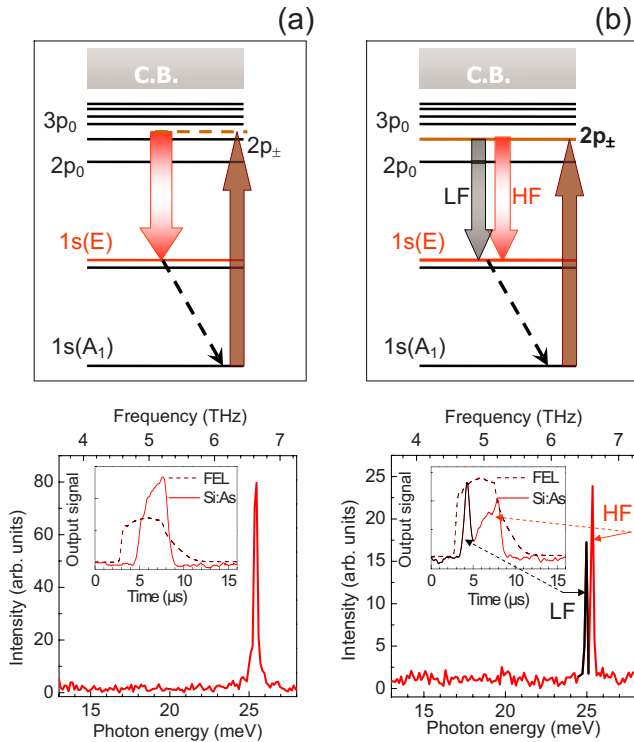


FIG. 1. (Color online) The two upper panels show the lasing mechanism for the Raman laser (left, arrow down) and the combined donor (LF, arrow down) and Raman laser; LF and HF indicate the low-frequency and high-frequency contributions in the laser emission spectrum (b). C. B. designates the conduction band. Two lower graphs show typical Raman laser spectra and pulse dynamics (insets) at maximal pump power and different pump photon energies: (a) pure Raman lasing; with a FWHM  $\sim 0.17 \text{ cm}^{-1}$ . The Raman laser pulse has a  $1.7 \mu\text{s}$  delay relative to the pump macropulse. Pumping is in between the  $2p_{\pm}$  and  $3p_0$  excited states. (b) Combined Raman and donor lasing: the donor lasing develops faster and has a shorter delay relative to the pump macropulse. Pumping is in vicinity of the  $2p_{\pm}$  state.

can be attributed to Stokes-shifted Raman emission. The Raman emission pulse has a  $\sim 2 \mu\text{s}$  delay with respect to the FEL macropulse [Fig. 1(a), inset]. Pumping into the  $2p_{\pm}$  state with a photon energy of  $47.69 \text{ meV}$  results in a double

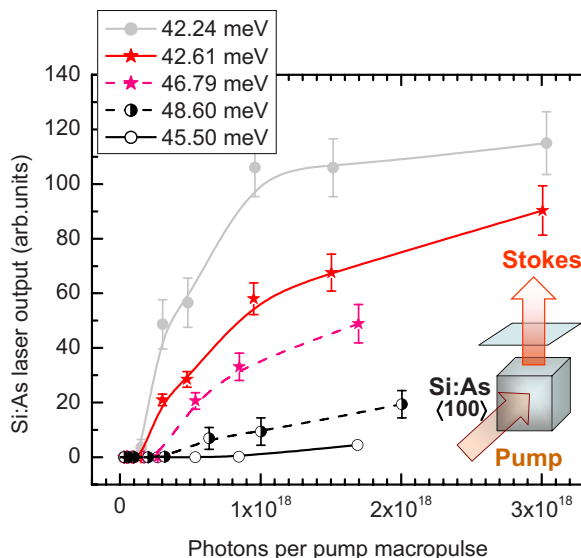


FIG. 2. (Color online) Dependences of the Si:As laser emission on the photon number per FEL macropulse. The laser intensity value is integral over entire pulse duration. The stars indicate Raman lines. The pump photon energies are given in the upper left corner. A sketch of the experimental setup is shown in the lower right corner.

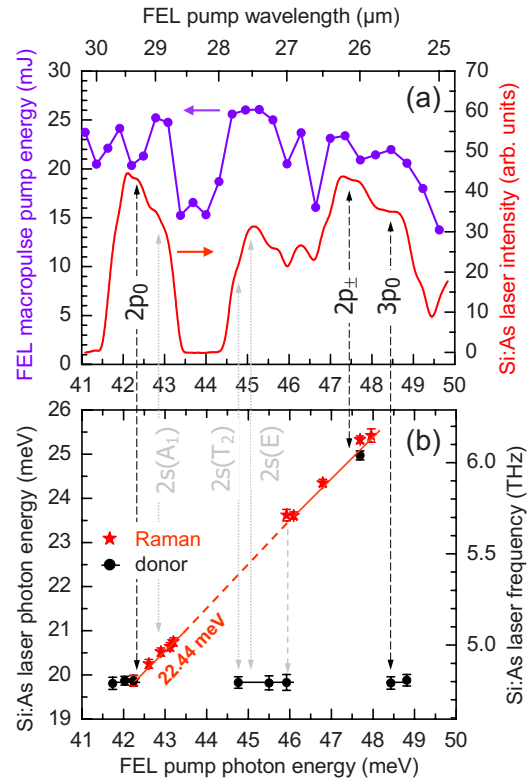


FIG. 3. (Color online) Overview of the frequency band generated in optically pumped Si:As. (a) FEL pump spectrum at maximal power (upper graph, low resolution scan). The laser intensity value is integral over last  $3 \mu\text{s}$  (gate is set to  $5.5\text{--}8.5 \mu\text{s}$  as in Fig. 1) of the emission pulse. The dip between  $43.5$  and  $44.5 \text{ meV}$  is due to strong waver vapor absorption. The Si:As emission spectrum (lower graph) shows a correlation between the maximum output intensity and the energy of the donor states. (b) Frequency bands covered by Raman and donor Si:As laser schemes. The Stokes shift in the Raman emission is  $22.44 \text{ meV}$ . The error bar shows the FWHM of the laser lines.

peak emission spectrum [Fig. 1(b)] as well as a double peak emission pulse [Fig. 1(b), inset]. The delay between pump and emission pulse is about  $1 \mu\text{s}$  for the first part of the emission pulse and about  $2 \mu\text{s}$  for the second part. The emission spectrum consists of two peaks, the low frequency (LF) peak fits to the intracenter  $2p_{\pm} \rightarrow 1s(E)$  transition at  $6.0 \text{ THz}$  ( $24.9 \text{ meV}$ ), while the second, high frequency (HF) peak fits to the Stokes emission.

In Fig. 2 the output power of the Si:As laser is shown as a function of pump photon number. The pump photon number of the threshold as well as the maximum output power depend on the pump photon energy. This is typical for terahertz silicon lasers. Laser emission occurs for a broad range of pump photon energies between  $\sim 42$  and  $\sim 49 \text{ meV}$  [Fig. 3(a)] corresponding to pumping into the  $2p_0$  state up to pumping into the  $3p_0$  state. Plotting the laser emission frequency as a function of the pump photon energy yields a linear dependence according to (Fig. 3)

$$\hbar\omega_S = \hbar\omega_{\text{FEL}} - (22.44 \pm 0.04 \text{ meV}). \quad (1)$$

The energy of the emission photon  $\hbar\omega_S$  is Stokes-shifted from the pump photon energy,  $\hbar\omega_{\text{FEL}}$ , by  $\Delta E = 22.44 \pm 0.04 \text{ meV}$  ( $5.42 \text{ THz}$ ). This fits very precisely to the interstate energy gap between the arsenic ground state [ $1s(A_1)$ , binding energy  $E_{1s(A_1)} = 53.76 \text{ meV}$  (Ref. 16)] and the split-off doublet state [ $1s(E)$ ,  $E_{1s(E)} = 31.34 \text{ meV}$  (Ref. 14)]. It is in agreement with the earlier finding that only one

valley-orbit Raman transition, namely the  $1s(A_1)$ - $1s(E)$  donor electronic transition, occurs in silicon.<sup>17</sup>

The Stokes emission ceases in the pump photon energy band from 43.4 to 45.9 meV (Fig. 3). In the range from 43.4 to 44.5 meV it does not appear because of insufficient pump power, which drops due to strong water absorption in this frequency range. Pumping in the band from 44.5 to 45.9 meV results in the regular donor laser emission (transition  $2p_0 \rightarrow 1s(E)$  at 18.9 meV or 4.8 THz). This lasing has the largest optical threshold (Fig. 2). It is worth noting that the  $2p_{\pm} \rightarrow 1s(E)$  laser transition is dominant under pumping into the  $2p_{\pm}$  state due to a low-efficient relaxation chain  $2p_{\pm} \rightarrow 2s \rightarrow 2p_0$  in Si:As (Ref. 15) caused by a fast depletion of the  $2s$  state via interaction with a longitudinal acoustic  $f$ -LA intervalley phonon. The donor type lasing process under pumping in the band from 44.5 to 45.9 meV indicates that the pump radiation terminates in the  $2s$  arsenic state. Theoretical simulation of the As donor state spectrum<sup>18</sup> yields the values of  $E_{2s(E)} \approx 8.76$  meV,  $E_{2s(T_2)} \approx 9.01$  meV, and  $E_{2s(A_1)} \approx 10.9$  meV [corresponding photon energies for the pump transitions are (Fig. 3):  $\hbar\omega_{\rightarrow 2s(E)} \approx 45.0$  meV,  $\hbar\omega_{\rightarrow 2s(T_2)} \approx 44.75$  meV, and  $\hbar\omega_{\rightarrow 2s(A_1)} \approx 42.86$  meV]. This indicates that the  $1s(A_1) \rightarrow 2s$  arsenic transition can be considered as a pump mechanism at large FEL intensities despite the fact that it is optically dipole-forbidden. The excitation is followed by the relaxation step  $2s \rightarrow 2p_0$  and further laser emission from  $2p_0 \rightarrow 1s(E)$  transition. It is worth noting that the strongest Stokes lasing appears under pumping in the vicinity of donor states ( $2p_0$  and  $2p_{\pm}$ ) where conditions of the “incoming” resonant scattering occur (Fig. 1).

Stimulated Raman emission (Fig. 2) has been reached at an FEL flux above  $10^{17}$  photons per pump macropulse (the lowest threshold per macropulse of about 0.6 mJ at 42.61 meV) that corresponds to a micropulse peak intensity of approximately 13 kW/cm<sup>2</sup> at a pump photon energy of 42.61 meV. This threshold is similar to the values obtained for the best Si:Sb Raman lasers.<sup>10</sup> The output power of the Si:As Raman laser in the pulse peak is a few milliwatts at maximum pump power (maximum pump pulse peak  $\sim 1$  MW). The “pulsed” gain coefficient  $\gamma_S$  can be estimated by considering lifetime of radiation in the cavity ( $\sim 15$  ns), which is relatively long compared to the train period of the micropulse (1 ns), and cavity losses of  $\sim 0.01$  cm<sup>-1</sup>. This yields a value of  $\gamma_S \approx 2.48$  cm MW<sup>-1</sup>. The pulsed gain for the Raman lasing, therefore, becomes comparable with the gain for the donor lasing [ $\sim (5-10)$  cm<sup>-1</sup> Ref. 19] at pump intensities above  $\sim 1$  MW/cm<sup>2</sup>.

In conclusion, we have demonstrated stimulated Stokes emission from a Raman laser based on intracenter transitions in silicon crystals doped by arsenic donors. The Stokes shift in the Si:As laser emission is determined by the Raman-active transition  $1s(A_1)$ - $1s(E)$  of the arsenic donor. Raman lasing has been found in a relatively broad frequency range, if compared with Si:P Raman lasers. The lowest lasing threshold of  $\sim 13$  kW/cm<sup>2</sup> was obtained for pumping in vi-

cinity of the  $2p_0$  state. In addition, weak donor lasing has been observed when pumping with photon energies close to the  $2s(E)$  state.

This work was partly supported by the Deutsche Forschungsgemeinschaft (DFG) (Project No. 436 RUS 113/937/0-1), by the Russian Foundation for Basic Research (RFBR-DFG) (Grant Nos. 02-08-91951, RFBR 08-00333), and the European Commission through the Research Infrastructure Action under the FP6 “Structuring the European Research Area” Programme through the Integrated Infrastructure Initiative “Integrating Activity on Synchrotron and Free Electron Laser Science” and the PROFIT program of the Investitionsbank Berlin. We acknowledge the support by the Stichting voor Fundamenteel Onderzoek der Materie (FOM) in providing the required beam time on FELIX.

<sup>1</sup>A. Borak, *Science* **308**, 638 (2005).

<sup>2</sup>S. A. Lynch, D. J. Paul, P. Townsend, G. Matmon, Z. Suet, R. W. Kelsall, Z. Ikonc, P. Harrison, J. Zhang, D. J. Norris, A. G. Cullis, C. R. Pidgeon, P. Murzyn, B. N. Murdin, M. Bain, H. S. Gamble, M. Zhao, and W.-X. Ni, *IEEE J. Sel. Top. Quantum Electron.* **12**, 1570 (2006).

<sup>3</sup>L. Lever, A. Valavanis, Z. Ikonc, and R. W. Kelsall, *Appl. Phys. Lett.* **92**, 021124 (2008).

<sup>4</sup>H.-W. Hübers, S. G. Pavlov, and V. N. Shastin, *Semicond. Sci. Technol.* **20**, S211 (2005).

<sup>5</sup>P.-C. Lv, R. T. Troeger, T. N. Adam, S. Kim, J. Kolodzey, I. N. Yassievich, M. A. Odnoblyudov, and M. S. Kagan, *Appl. Phys. Lett.* **85**, 22 (2004).

<sup>6</sup>T. V. Altukhov, E. G. Chirkova, V. P. Sinis, M. S. Kagan, Yu. P. Gousev, S. G. Thomas, K. L. Wang, M. A. Odnoblyudov, and I. N. Yassievich, *Appl. Phys. Lett.* **79**, 3909 (2001).

<sup>7</sup>S. A. Lynch, R. Bates, D. J. Paul, D. J. Norris, A. G. Cullis, Z. Ikonc, R. W. Kelsall, P. Harrison, D. D. Arnone, and C. R. Pidgeon, *Appl. Phys. Lett.* **81**, 1543 (2002).

<sup>8</sup>S. G. Pavlov, R. Kh. Zhukavin, E. E. Orlova, V. N. Shastin, A. V. Kirsanov, H.-W. Hübers, K. Auen, and H. Riemann, *Phys. Rev. Lett.* **84**, 5220 (2000).

<sup>9</sup>V. N. Shastin, R. Kh. Zhukavin, E. E. Orlova, S. G. Pavlov, M. H. Rümmele, H.-W. Hübers, J. N. Hovenier, and T. O. Klaassen, *Appl. Phys. Lett.* **80**, 3512 (2002).

<sup>10</sup>S. G. Pavlov, H.-W. Hübers, J. N. Hovenier, T. O. Klaassen, D. A. Carder, P. J. Phillips, B. Redlich, H. Riemann, R. Kh. Zhukavin, and V. N. Shastin, *Phys. Rev. Lett.* **96**, 037404 (2006).

<sup>11</sup>S. G. Pavlov, H.-W. Hübers, U. Böttger, R. Kh. Zhukavin, V. N. Shastin, J. N. Hovenier, B. Redlich, N. V. Abrosimov, and H. Riemann, *Appl. Phys. Lett.* **92**, 091111 (2008).

<sup>12</sup>O. Boyraz and B. Jalali, *Opt. Express* **12**, 5269 (2004).

<sup>13</sup>H. Rong, A. Liu, R. Jones, O. Cohen, D. Hak, R. Nicolaescu, A. Fang, and M. Paniccia, *Nature (London)* **433**, 292 (2005); H. Rong, R. Jones, A. Liu, O. Cohen, D. Hak, A. Fang, and M. Paniccia, *ibid.* **433**, 725 (2005).

<sup>14</sup>H.-W. Hübers, S. G. Pavlov, H. Riemann, N. V. Abrosimov, R. Kh. Zhukavin, and V. N. Shastin, *Appl. Phys. Lett.* **84**, 3600 (2004).

<sup>15</sup>S. G. Pavlov, H.-W. Hübers, P. M. Haas, J. N. Hovenier, T. O. Klaassen, R. Kh. Zhukavin, V. N. Shastin, D. A. Carder, and B. Redlich, *Phys. Rev. B* **78**, 165201 (2008).

<sup>16</sup>A. K. Ramdas and S. Rodriguez, *Rep. Prog. Phys.* **44**, 1297 (1981).

<sup>17</sup>G. B. Wright and A. Mooradian, *Phys. Rev. Lett.* **18**, 608 (1967).

<sup>18</sup>Y.-C. Chang, T. C. McGill, and D. L. Smith, *Phys. Rev. B* **23**, 4169 (1981).

<sup>19</sup>R. Kh. Zhukavin, V. N. Shastin, S. G. Pavlov, H.-W. Hübers, J. N. Hovenier, T. O. Klaassen, and A. F. G. van der Meer, *J. Appl. Phys.* **102**, 093104 (2007).